

# Frequency-multiplexed image storage and conversion in a cold atomic ensemble

Dong-Sheng Ding<sup>†</sup>, Jing-Hui Wu, Zhi-Yuan Zhou, Bao-Sen Shi<sup>\*</sup>, Xu-Bo Zou, and Guang-Can Guo

Key Laboratory of Quantum Information, University of Science and Technology of China, Hefei 230026, China

Corresponding author: <sup>\*</sup>[drshi@ustc.edu.cn](mailto:drshi@ustc.edu.cn)

<sup>†</sup>[dds@mail.ustc.edu.cn](mailto:dds@mail.ustc.edu.cn)

## Abstract

The strong demand for quantum memory, a key building block of quantum network, has inspired new methodologies and led to experimental progress for quantum storage. The use of quantum memory for spatial multimode or image storage could dramatically increase the channel bit-rate. Furthermore, quantum memory that can store multiple optical modes would lead to higher efficiencies in quantum communication and computation. Here, by using resonant tripod electromagnetically induced transparency in a cold atomic ensemble, we experimentally demonstrate frequency-multiplexed quantum image memory at near the single-photon level, where two probe fields have discrete wavelengths and different spatial information. In addition, by using different read-light, we realize linear frequency conversion of retrieved images, the efficiency is much high compared with previous reported works, where such a conversion is achieved through weak nonlinear effect. Besides, our method could be used to create a superposition of the images by realizing the function of a beamsplitter. These advantages make our method very useful in many fields including quantum information, detection, imaging, sensing, night-vision and even astrophysical observation.

## Introduction

A long-distance quantum communication network consists of a memory in which quantum information can be stored and manipulated at will and a carrier via which the different memories can be connected and exchange quantum information. The seminar work of Duan *et. al.* [1] shows that an atomic system could be a suitable candidate for the memory and that the different memories could be connected through a photon, a robust and efficient carrier of quantum information due to its weak interaction with the environment.

The strong demand for quantum memory has inspired new methodologies and led to experimental progress for quantum storage using an atomic system via different mechanisms, for example, electromagnetically induced transparency (EIT) [2, 3], atomic frequency combs [4, 5], Raman schemes [6, 7], and gradient echo memory [8, 9], etc. Even so, there has been little progress on spatial multimode or image storage.

A quantum memory which could store spatial multimode or images is very useful because it allows for simultaneous storage of multiple signals in a single storage device. It could dramatically increase the channel bit-rate. Recently there has been some progress related to the storage of images. In Ref. 10-12, images were stored via EIT in a hot atomic ensemble or a doped solid. In Ref. 13 and 14, the four-wave mixing technique was used to store an image in a hot or cold atomic ensemble. Very recently, the spatial mode storage in gradient echo memory was realized in a hot atomic ensemble [15]. Additionally, quantum memories that are able to store multiple optical modes offer advantages over single-mode memories in terms of speed and robustness – advantages that can, in turn, lead to higher efficiencies in quantum communication and computation experiments [16, 17]. There has been some experimental research in this direction, such as storing multiple modes using the gradient echo memory scheme in a hot atomic ensemble [8] or using the technique of the spectral shaping of an inhomogeneously broadened optical transition into an atomic frequency comb in solids doped with rare earth metal ions [4]. Very recently, we reported the experimental demonstration of storage and retrieval of multimode images in the spatial domain through EIT in a cold <sup>85</sup>Rb atomic cloud [18]. So far, there had been no reports on the storage of multimode images in frequency domains.

A promising way of storing multiple optical modes is to store the different optical modes in different atomic collective spin excitation states, which could, for example, be realized by a tripod configuration of atoms. There has been some related progress along this direction of research, for example, in Refs. 19 and 20, where dual-channel memory for storing a qubit (no image) using a tripod configuration via EIT was realized. In this paper, we report the experimental evidence that two different images can be stored in the frequency domain using a tripod EIT configuration in a cold atomic ensemble. Furthermore, by using different read-light, we realize the highly-efficient frequency conversion of the stored images and could therefore control the wavelength of the output images. One interesting point we want to emphasize is that the frequency conversion of image is based on a first-order linear effect, neither a second-order effect like difference frequency down-conversion with a nonlinear crystal nor a third-order effect like nonlinear four-wave mixing using atoms, therefore the conversion efficiency is very high, about 3 orders higher than that achieved in a recent upconversion experiment by the three-order effect in a hot atomic ensemble [21, 22], is also much higher than that (about 13%) obtained by intracavity four-wave mixing in nonlinear Fabry-Perot interferometer [23] and is also higher than that (40%) obtained through a three-wave mixing process in a cavity by using a high power solid laser [24]. We believe that such technique will find wide applications in detection, imaging, sensing, night-version and even astrophysical observation. It is also useful for building up a high dimensional quantum repeater in the future. Besides, we could create the superposition of the two images by realizing the function of a beamsplitter, which is the key element of quantum information processing. We could realize two different superposition images states: one is superposition state of the

leaked part and the retrieved part without frequency conversion, another is the superposition state consisted of the leaked part with and the retrieved part with frequency-converted wavelength. The frequency-multiplexed quantum image memories accompanied by quantum frequency conversion are very promising for quantum communication in the future.

We consider the state of input probe fields as expressed in the following:

$$\psi_{input} = |\lambda_1\rangle|I_1\rangle + |\lambda_1'\rangle|I_2\rangle \quad (1)$$

where,  $\lambda_{1,2}$  indicate wavelength,  $I_{1,2}$  describe spatial information,  $|\lambda_1\rangle|I_1\rangle$  and  $|\lambda_1'\rangle|I_2\rangle$  describe input probes 1 and 2 with wavelengths  $\lambda_1$  and  $\lambda_1'$ , respectively. The frequency shift between these two probe fields is defined as  $\Delta$ . If we use the  $\lambda_1$  field as read-light, then the retrieved probe 1, 2 fields are expressed as:

$$\psi_{output} = \sqrt{\eta_1}|\lambda_1\rangle|I_1\rangle + \sqrt{\eta_2}|\lambda_1'\rangle|I_2\rangle \quad (2)$$

where,  $\sqrt{\eta_1}|\lambda_1\rangle|I_1\rangle$  describes retrieved probe 1 at  $\lambda_1$  with storage efficiency of  $\eta_1$ ,  $\sqrt{\eta_2}|\lambda_1'\rangle|I_2\rangle$  corresponds to retrieved probe 2 at  $\lambda_1'$  with storage efficiency of  $\eta_2$ . If we apply a  $\lambda_2$  field as read-light, then the readout probe fields can be described by:

$$\psi_{output} = \sqrt{\eta_3}|\lambda_2\rangle|I_1\rangle + \sqrt{\eta_4}|\lambda_2'\rangle|I_2\rangle \quad (3)$$

where,  $\sqrt{\eta_3}|\lambda_2\rangle|I_1\rangle$  describes retrieved probe 1 at  $\lambda_2$  with conversion efficiency of  $\eta_3$ ; and  $\sqrt{\eta_4}|\lambda_2'\rangle|I_2\rangle$  corresponds to retrieved probe 2 at  $\lambda_2'$  with conversion efficiency of  $\eta_4$ . The frequency shift between  $\lambda_2$  and  $\lambda_2'$  is still  $\Delta$ . The frequencies of retrieved probes are converted in comparison with Eq. (2) and (3)

### Experimental configuration


Figure 1 shows the experimental setup. Two laser beams are modulated by a sequence of acousto-optic modulators (AOMs) to generate two probe fields, one write (W) field and two read (R, R') fields. In our experiment, a tripod (EIT) configuration shown in Fig. 1b was used to perform the storage experiment. A cigar-shaped atomic cloud of  $^{85}\text{Rb}$  atoms is used as the storing media. The probe fields and the W(R) beam from the external-cavity diode laser (DL100, Toptica) have the same wavelength of 795-nm. The probe fields were imprinted with a real image through a mask: a standard resolution chart (USAF target). The R' beam from the external-cavity diode laser (DL100, Toptica) has the wavelength of 780-nm. Probe 1 ( $P_1$ ) and the W(R) fields are resonant with the transitions  $5S_{1/2}(F=3) |2\rangle \rightarrow 5P_{1/2}(F'=2) |4\rangle$  and  $5S_{1/2}(F=3) |1\rangle \rightarrow 5P_{1/2}(F'=2) |4\rangle$ , respectively. Probe 2 ( $P_2$ ) is resonant with the transition  $5S_{1/2}(F=2) |3\rangle \rightarrow 5P_{1/2}(F'=2) |4\rangle$ . And the R' field is resonant with the transition  $5S_{1/2}(F=3) |1\rangle \rightarrow 5P_{3/2}(F'=3) |5\rangle$ . We used two photomultiplier tubes (PMT) (Hamamatsu, H10721) to detect probe fields in the time domain and used a time-resolution camera to monitor spatial information. By adjusting a quarter-wave plate before the MOT, the coupling and probe fields were assigned opposite circular polarizations. Using a quarter-wave plate after the MOT, the fields were later reversed to have orthogonal linear polarizations.

We used a resonant tripod EIT configuration shown in figure 1(b). A cigar-shaped atomic cloud of  $^{85}\text{Rb}$  atoms was obtained in a two-dimensional magneto-optical trap (MOT) and served as the memory element in our experiment. The non-degenerate states  $|2\rangle$  and  $|3\rangle$  were used in our system. We used a 1.5 GHz AOM to generate probe 2 with double-pass light and a frequency shift of 3.0378 GHz relative to probe 1 or the R field. Input signals were modulated into Gaussian profiles by an arbitrary signal generator (AFG 3252). A high time-resolution camera (1024×1024, iStar 334T series, Andor) was used to monitor the spatial structure of the probe fields, including a sequence of leakage pulses and retrieved pulses. The camera has a quantum efficiency of approximately 25% at 795 and 780nm. The camera with its high speed shutter could be triggered by an external TTL signal. This TTL signal was generated from AFG 3252 and delayed by a delay generator (DG 535). The total size of the camera sensor was 13.3×13.3mm. Our geometry was based on a 4-f imaging system, consisting of the center plane of the atomic cloud, the imaging plane of the camera, the mask plane, and the two lenses. L1 and L2 are lenses with a focal length of 300mm and 500mm, respectively. In our experiment, the repump light was turned off before cooling light by 30μs, allowing the atoms to decay into the ground states  $|2\rangle$  and  $|3\rangle$  and balanced for preparation of the initial states. In our experiment, the full input pulse was divided equally into two parts. One part was stored and the other part was leaked. The conversion efficiency was calculated by ratio between the powers of retrieved signal and the leaked pulse.

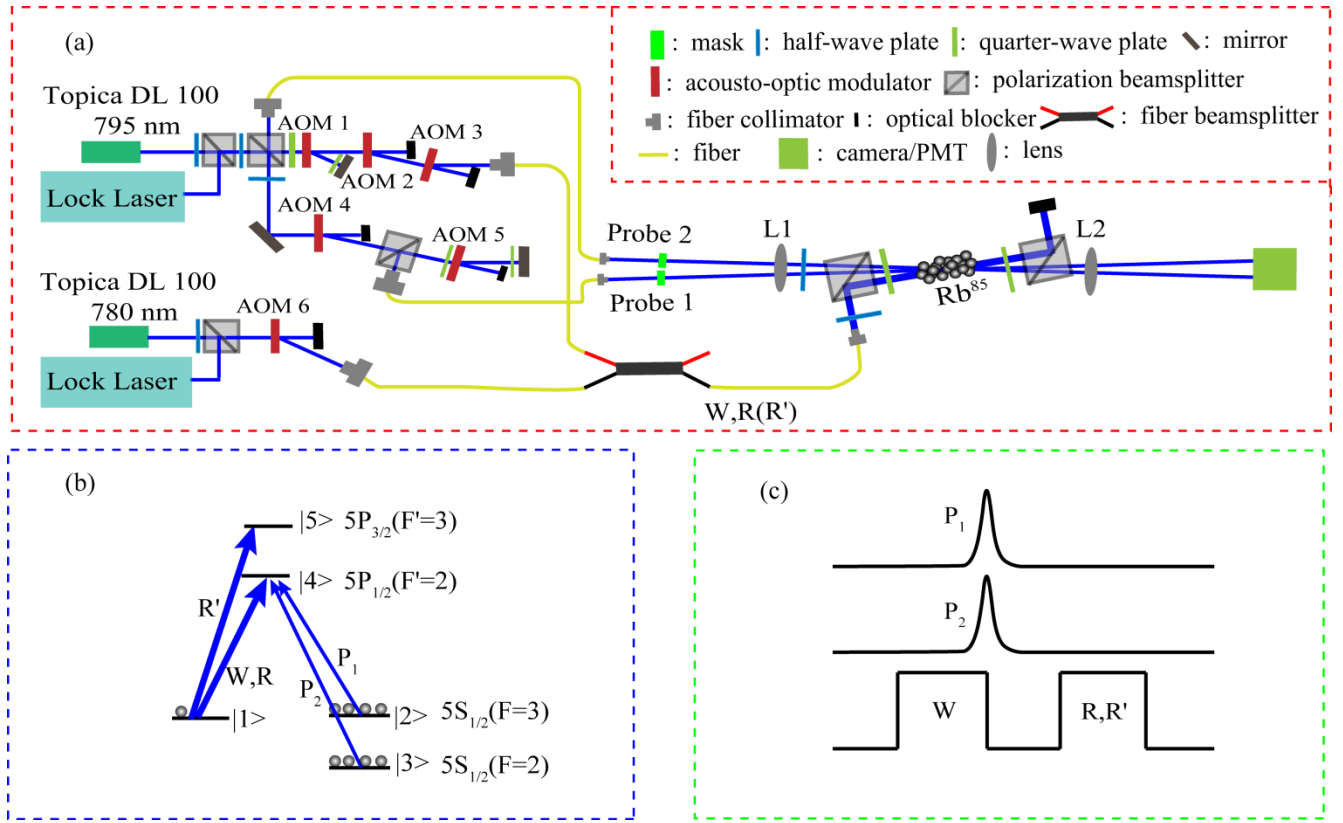


**Figure 1 Tripod image storage using cold atom.** (a) Experimental setup. The frequency of probe 1 ( $P_1$ ) is shifted by AOM 4 (frequency shift 160 MHz) and AOM 5 (double-pass frequency shift -160 MHz); The frequency of probe 2 ( $P_2$ ) is shifted by AOM 1 (double-pass frequency shift 3.0378 GHz); The frequency of W(R) is shifted by AOM 2 (frequency shift 80 MHz) and AOM 3 (frequency shift -80 MHz); The read beam  $R'$  is from another laser and is modulated by AOM 6.  $P_1$  and  $P_2$  propagate with a small angle  $0.1^\circ$ . The angle between  $P_1$  and the read beam is about  $1.8^\circ$ . The non-collinear configuration used in the experiment significantly reduces the noise from the coupling scattering. (b) Experimental energy diagram. (c) Timing sequence. Probe fields are modulated by acousto-optic modulators to form a Gaussian pulse sequence. The W field writes the probe fields into the atomic collective spin excitation state and the R,  $R'$  fields read them out.

## Experimental results

We take the parameters to be as follows:  $\lambda_1=795$  nm,  $\lambda_1'=795$  nm (the frequency shift between the probe fields is  $\Delta=3.0378$  GHz);  $I_1$  describes the spatial information of the digit “2”; and  $I_2$  describes the spatial information of the image “”. The wavelength of R is  $\lambda_1=795$  nm. The power of the W(R) field is  $30\mu\text{W}$  and the  $R'$  field is  $140\mu\text{W}$ . The W(R) field and  $R'$  field are 3 mm in diameters and cover the probe beams completely. If we use the R field as read-light, the retrieved signals have a wavelength of 795nm due to the tripod EIT configuration. The signals obtained by PMTs are shown in figure 2(a), the probes 1 and 2 are retrieved after about  $4.5\mu\text{s}$  long storage time. The storage efficiency of probe 1 is  $\eta_1=0.22$ , the storage efficiency of probe 2 is  $\eta_2=0.24$ . Then, we change the PMTs to the high-resolution camera for detecting spatial information. By properly adjusting the delay of the synchronization signal (the trigger delay can be adjusted by the camera itself or by using a delay generator (DG 535)), we can obtain the maximal intensity of leakage images and the retrieved images. The results are shown in figure 2(b). The left column corresponds to the storage of probe 1 and the middle column is the storage of probe 2. The case of probe 1 and probe 2 being simultaneously stored and retrieved is shown in the right column of Figure 2(b). There is almost no difference between the leakage images and the retrieved images. We conclude that there is no crosstalk between the storage of probe 1 and probe 2.

By using an attenuator, we reduced the intensity of the probe fields and detected the leakage and retrieved images. There are about  $1.3 \times 10^3$  photons per pulse being stored. We obtained the results shown in figure 3; the retrieved images are very similar to the leaked images. We believe that the scheme could work at the single-photon level if we increase the density of the atoms and the repetition rate of the probes further. Very recently, a single-photon level image storage experiment has been done in our lab [18]. In that experiment, a high repetition rate for probe fields and the coupling field is employed, which leads to a high signal-to-noise ratio (SNR) at the single-photon level.

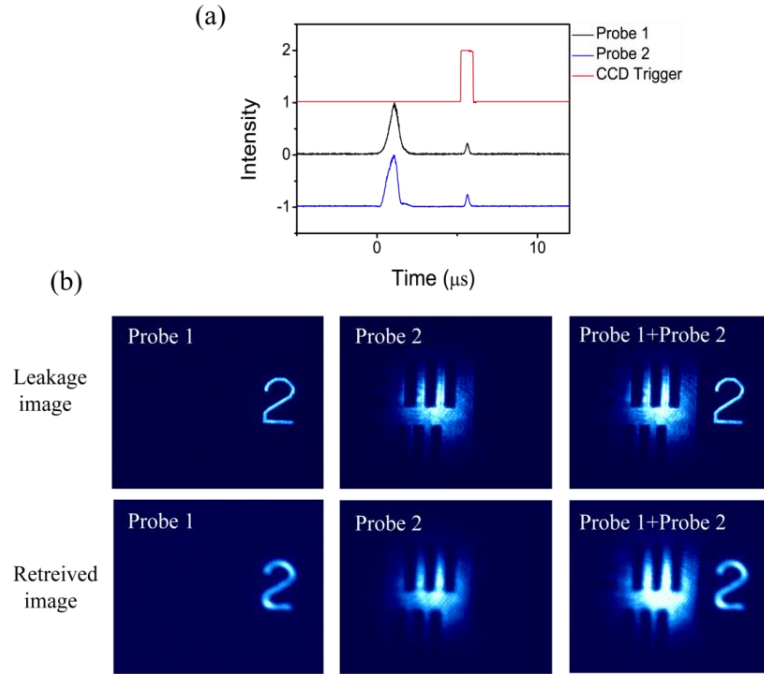


**Figure 2 Leakage and the retrieved signal using the R field as read-light.** (a) The intensity of the leakage and retrieved probe fields recorded by two PMTs. The black line is probe 1 and the blue line is probe 2. The red line is a trigger signal for the camera shutter (CCD). (b) The leakage and retrieved images were recorded by a high-resolution camera. Each image is the sum of the 200 retrieved images. The exposure time of the CCD camera was 1.0 s.

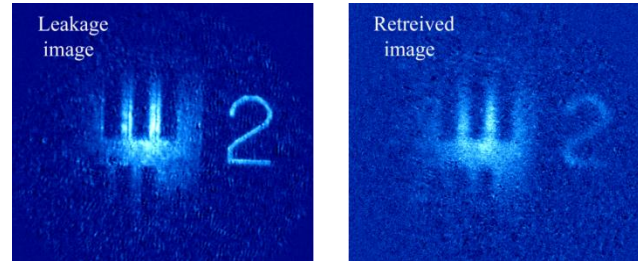


**Figure 3 Leakage and the retrieved images using the R field as read-light near single-photon level.** The left column is the leakage image; the right column is the retrieved image. Each image is the sum of the 200 retrieved images. The exposure time of the CCD camera was 1.0 s.

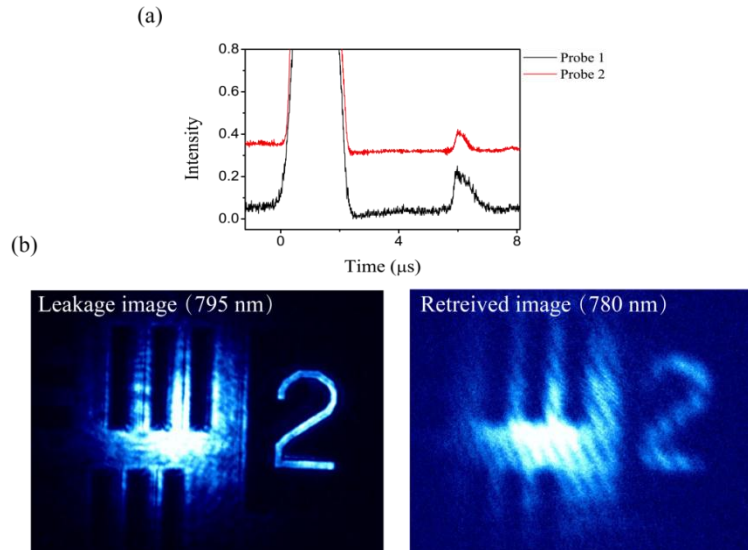


**Figure 4 Leakage and the retrieved image using the R' field as read-light.** Figure 4(a) is the intensity signal in the time domain recorded by PMTs. The left column of figure 4(b) is the leakage image with a wavelength of 795nm; right column is the retrieved image with a wavelength of 780nm.

Each image is the sum of the 200 retrieved images. The exposure time of the CCD camera was 1.0s.

Next, we want to see what will happen if a different read-light  $R'$  with different wavelength is used. In order for that to occur, we use the  $R'$  field with a wavelength of  $\lambda_2=780\text{nm}$  as our read-light, with results in the time domain as shown in figure 4(a). The leakage signals have a wavelength of  $795\text{nm}$ , but the retrieved signals have a wavelength of  $780\text{nm}$ ! Therefore we realize the image storage and its frequency conversion in a storage device! The frequency conversion efficiency of probe 1 is  $\eta_3=0.012$ , the efficiency of probe 2 is  $\eta_4=0.067$ . Figure 4(b) is a record of the spatial structures of retrieved probes using the camera. In this case, we reduced the intensity to be at nearly the single-photon level: there are about  $6 \times 10^5$  photons per pulse being stored. The image information is retrieved after  $4.5\mu\text{s}$  long storage time. The experimental results show that the frequency of the output fields can be changed using different read-light and the spatial information of the probe fields will still be preserved.

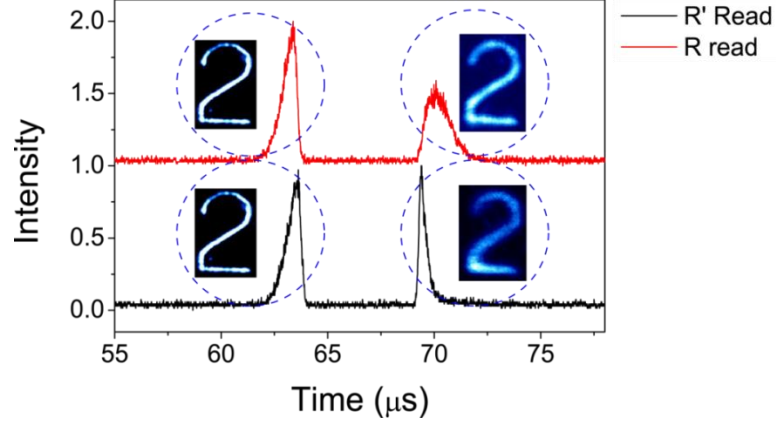


**Figure 5 The frequency conversion of images through EIT.** The red line is using the  $R$  field as read-light; the black line is using the  $R'$  field as read-light. Both lines are obtained by PMTs. The write fields are both  $W$  fields. The images in upper line are leakage and retrieved image with  $R$  field as read-light, the images on down line are leakage and retrieved image with  $R'$  field as read-light.

The experiment shown before has clearly demonstrated that a tripod configuration of atoms could be used to realize frequency conversion of images. For such as a process, the frequency conversion efficiency and the similarity between the frequency-converted image and the input image are important parameters for evaluating its workability. In the following, we checked the frequency conversion efficiency in the image memory. We only used the degenerate  $\Lambda$ -EIT configuration to convert the  $795\text{ nm}$  light to  $780\text{ nm}$  light; the result is shown in figure 5. In the experiment, we used the  $W$  field to write probe 1 imprinted with digit "2" into the atomic ensemble. The number of photons in the probe 1 was about one thousand per pulse. When we employed the  $R$  field to read out the storage field, the red line in figure 5 was the result and the efficiency of the storage was about 0.91. Then, we used the  $R'$  field to read out the storage field, the wavelength of the probe 1 field is converted to be  $780\text{ nm}$ , and the black line in figure 5 is the result. The efficiency of this conversion is about 0.74. Even the number of photons of each probe pulse is reduced to be less than 10 photons, the efficiency still keeps high as about 0.7. By applying same method shown in Ref. [18], we calculated the similarity between the leaked image and the retrieved image, which are about 83% and 79% corresponding to using  $R$  and  $R'$  read-light respectively. The difference in pulse width between the retrieved signals in figure 5 is caused by different powers of the read pulses [25], the width of the retrieval is inversely proportional to the intensity of the reading field. In our experiment, the power of  $R$  field is about  $30\mu\text{W}$  and the power of  $R'$  field is about  $0.6\text{ mW}$ , therefore the width of retrieval by  $R$  field is large than that by  $R'$  field.

## Discussion and analysis

The retrieved images are very similar to the input images, even when different read-lights are used. This illustrates that the spatial properties  $|I_j\rangle$  in state  $|\lambda_n\rangle|I_j\rangle$  do not change during the process of storing and retrieving, and the process of frequency conversion. Moreover, the readout images between the probe fields have no crosstalk between them. In figure 3, there are about  $1.3 \times 10^3$  photons per pulse being stored, which is higher than the number of photons in Ref. [18]. In this experiment, the populations of the ground states we prepared needed to be balanced and the atomic populations in this tripod configuration are relatively small compared with the degenerate configuration in Ref. [18]. Therefore, the repetition of storage experiment per second is hard to increase. Otherwise, the populations are smaller and the storage efficiency is lower compared with the degenerate configuration. From figure 3 and 4, we observe that the input state  $\psi_{input} = \sum |\lambda_i\rangle|I_j\rangle$  is converted into the state  $\psi_{output} = \sum \sqrt{\eta_n} |\lambda_n\rangle|I_j\rangle$ , where  $(n, i, j) = (1, 2)$ . This process can be used to realize the function of a beamsplitter, by which the superposition of the different images at different wavelengths is obtained. This function is realized by storing only part of the probes, such that the leakage image and the retrieved image consist of the superposition [26]. We could realize two different superposition images states: one is superposition state of the leaked part and the retrieved part without frequency conversion,

another is the superposition state consisted of the leaked part with wavelength of  $\lambda_1$  and the retrieved part with the wavelength of  $\lambda_2$  when the frequency conversion is applied. In these cases shown above, we consider two probes separately. If we consider them simultaneously, then an entangled image state consisted of two leaked parts and two retrieved parts could be created. It is worth illustrating that this quantum frequency conversion is based on the EIT configuration. It is a linear effect rather than a second-order nonlinear effect like difference frequency generation using a nonlinear crystal or a third-order nonlinear effect like a four-wave mixing in an atomic system. Therefore the conversion efficiency is very high, about 3 orders higher than that achieved in a recent upconversion experiment by the three-order effect in a hot atomic ensemble [21, 22], is also much higher than that (about 13%) obtained by intracavity four-wave mixing in nonlinear Fabry-Perot interferometer [23] and is also higher than that (40%) obtained through a second-order nonlinear process by using a high power solid laser with the aid of a cavity [24]. By our method, we could realize the frequency conversion of images between different wavelength band, for example, if the energy level of 6p of the  $^{85}\text{Rb}$  atom is considered, then the image could be transferred from near infrared band (795 nm) to ultraviolet band (420 nm). We believe that such technique will find wide applications in detection, imaging, sensing, night-vision and even astrophysical observation. It is also useful for building up a high dimensional quantum repeater in the future.

In summary, we have experimentally demonstrated that frequency-multiplexed images can be stored and retrieved in a cold atomic ensemble using resonant tripod EIT configuration. The probe fields can be converted to different frequencies by applying different read-light while the spatial information is preserved. Our results are important for future quantum communication in high-dimensional quantum networks and other fields.

### Acknowledgments

This work was supported by the National Natural Science Foundation of China (Grant Nos. 10874171, 11174271), the National Fundamental Research Program of China (Grant No. 2011CB00200), and the Innovation fund from CAS, Program for NCET.

### Author contributions

BSS and XBZ conceived the experiment for discussion. The experimental work and data analysis were carried out by DSD and BSS, with assistance from JHW and ZYZ. BSS and DSD wrote this paper with assistance from JHW and ZYZ. BSS, XBZ and GCG supervised the project.

### References

1. Duan, L.-M., Lukin, M. D., Cirac, J. I. and Zoller, P., Long-distance quantum communication with atomic ensembles and linear optics, *Nature* 414, 413–418 (2001).
2. Fleischhauer, M. and Lukin, M. D., Dark-State Polaritons in Electromagnetically Induced Transparency, *Phys. Rev. Lett.* 84, 5094 (2000).
3. Phillips, D. F., Fleischhauer, M., Mair, A., Walsworth, R. L., and Lukin, M. M., Storage of Light in Atomic Vapor, *Phys. Rev. Lett.* 86, 783 (2001).
4. Afzelius, M., Simon, C., de Riedmatten, H. and Gisin, N., Multimode quantum memory based on atomic frequency combs, *Phys. Rev. A.*, 79, 052329 (2009).
5. de Riedmatten, H., Afzelius, M., Staudt, M. U., Simon, C., and Gisin, N., A solid-state light-matter interface at the single-photon level, *Nature*, 456, 773 (2008).
6. Rein, R. F., Michelberger, P., Lee, K. C., Nunn, J., Langford, N. K., and Walmsley, I. A., Single-Photon-Level Quantum Memory at Room Temperature, *Phys. Rev. Lett.* 107, 053603 (2011).
7. K. F. Reim, J. Nunn, V. O. Lorenz, B. J. Sussman, K. C. Lee, N. K. Langford, D. Jaksch and I. A. Walmsley, Towards high-speed optical quantum memories, *Nat. Photon.* 4, 218 (2010).
8. Hosseini, M., Sparkes, B. M., Campbell, G., Lam, P. K. and Buchler, B. C., High efficiency coherent optical memory with warm rubidium vapour, *Nature Comm.* 2, DOI: 174 (2011).
9. Hosseini, M., Campbell, G., Sparkes, B. M., Lam, P. K. and Buchler, B. C., Unconditional room-temperature quantum memory, *Nature Phys.* 7, 794 (2011).

10. Vudiyasetu, P. K., Camacho, R. M. and Howell, J. C., Storage and Retrieval of Multimode Transverse Images in Hot Atomic Rubidium Vapor, *Phys. Rev. Lett.* 100, 123903 (2008).
11. Shuker, M., Firstenberg, O., Pugatch, R., Ron, A. and Davidson, N., Storing Images in Warm Atomic Vapor, *Phys. Rev. Lett.* 100, 223601 (2008).
12. Heinze, G., Rudolf, A., Beil, F. and Halfmann, T., Storage of images in atomic coherences in a rare-earth-ion-doped solid, *Phys. Rev. A* 81, 011401(R) (2010).
13. Mariuno, A. M., Pooser, R. C., Boyer, V., and Lett. P. D., Tunable delay of Einstein–Podolsky–Rosen entanglement , *Nature*, 457, 859 (2009).
14. Wu, J., Ding, D., Liu, Y., Zhou, Z., Shi, B., Zou, X., and Guo, G., Storage and Retrieval of an Image Using Four-Wave Mixing System in Cold Atomic Ensemble, arxiv: physics. atom-ph /1204:0955v4.
15. Higginbottom, D. B., Sparkes, B. M., Rancic, M., Pinel, O., Hosseini, M., Lam, P. K., and Buchler, B. C., Spatial mode storage in a gradient echo memory, arxiv: 1204.3981v2.
16. Sangouard, N., Simon, C., Zhao, B., Chen, Y.-A., de Riedmatten, H., Pan, J.-W. and Gisin, N., Robust and efficient quantum repeaters with atomic ensembles and linear optics, *Phys. Rev. A* 77, 062301 (2008).
17. Simon, C., de Riedmatten, H., Afzelius, M., Sangouard, N., Zbinden, H. and Gisin, N., Quantum Repeater with Photon Pair Sources and Multimode Memories, *Phys. Rev. Lett.* 98, 190503 (2007).
18. Dong-Sheng Ding, Jing-Hui Wu, Zhi-Yuan Zhou, Yang Liu, Bao-Sen Shi, Xu-Bo Zou, and Guang-Can Guo, Multimode quantum image memory based on a cold atomic ensemble, arXiv:1204.1130.
19. Shujing Li, Zhongxiao Xu, Haiyan Zheng, Xingbo Zhao, Yuelong Wu, Hai Wang, Changde Xie, and Kunchi Peng, Coherent manipulation of spin-wave vector for polarization of photons in an atomic ensemble, *Phys. Rev. A* 84, 043430 (2011).
20. Hai Wang, Shujing Li, Zhongxiao Xu, Xingbo Zhao, Lijun Zhang, Jiahua Li, Yuelong Wu, Changde Xie, Kunchi Peng, and Min Xiao, Quantum interference of stored dual-channel spin-wave excitations in a single tripod system, *Phys. Rev. A* 83, 043815 (2011).
21. Dong-Sheng Ding, Zhi-Yuan Zhou, Bao-Sen Shi, Xu-Bo Zou, and Guang-Can Guo, Experimental upconversion of images, arxiv: 1203:6132v2.
22. Dong-Sheng Ding, Zhi-Yuan Zhou, Bao-Sen Shi, Xu-Bo Zou, and Guang-Can Guo, Image Transfer through Two Sequential Four-Wave Mixing in a Hot Atomic Vapour, *Phys. Rev. A* 85, 053815 (2012).
23. Ormachea, O; Romanov, O G; Tolstik, A L; Arce-Diego, J L; Fanjul-Vázquez, F; Pereda-Cubian, D, Frequency up-conversion of coherent images by intracavity nondegenerate four-wave mixing, *Opt. Expresses*, 14, 8298-8304 (2006).
24. Pedersen, Christian; Karamehmedovic, Emir; Dam, Jeppe Seidelin; Tidemand-Lichtenberg, Peter, Enhanced 2D-image upconversion using solid-state lasers, *Opt. Expresses*, 17, 20885-20890 (2009).
25. Yong-Fan Chen, Shih-Hao Wang, Chang-Yi Wang, and Itai A. Yu. Manipulating the retrieved width of stored light pulses. *Phys. Rev. A* 72, 053803 (2005)
26. K. F. Reim, J. Nunn, X.-M. Jin, P. S. Michelberger, T. F. M. Champion, D. G. England, K.C. Lee, N. K. Langford, I. A. Walmsley “Multi-pulse addressing of a Raman quantum memory: configurable beam splitting and efficient readout” arXiv:1203.2328v1.